Antiproton-Driven Magnetically Insulated Inertial Confinement Fusion (MICF) Propulsion System

Terry Kammash
Nuclear Engineering and Radiological Sciences
The University of Michigan
Ann Arbor, MI 48109

Presented at
NIAC Fellows Meeting
November 8 - 9, 1999
Atlanta, GA 30318

Presentation Outline

1. What is MICF Propulsion and How It Works

2. Comparison with Implosion-Type Inertial Confinement Fusion (ICF)

3. Mathematical Plasma Modeling and Basic Equations

4. Classical and Anamolous Cross Field Transport

5. Preliminary Results and Fusion Energy gain

6. Application to Propulsion

7. Phase II Proposed Investigation

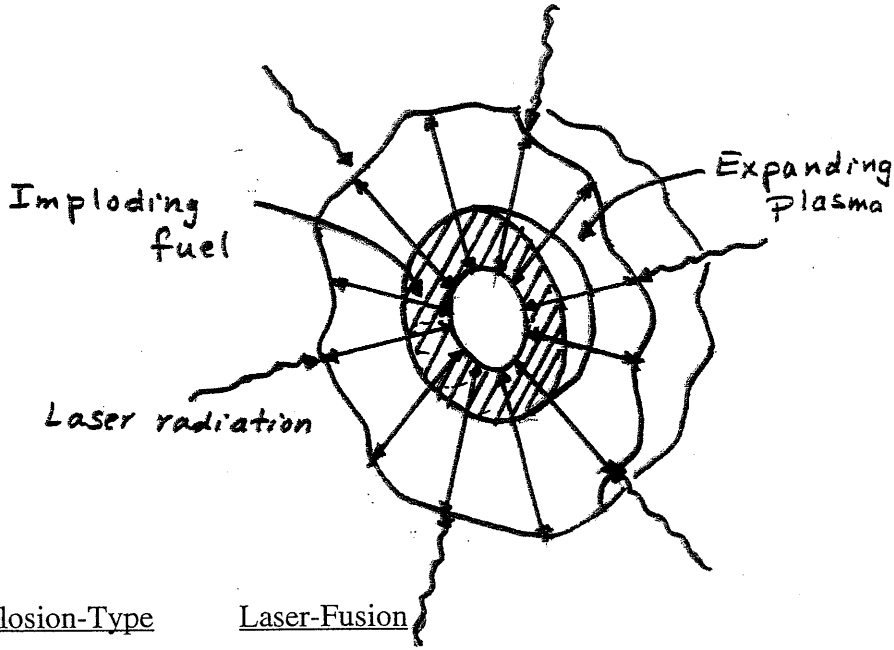

Implosion-Type Laser-Fusion

Major Issues

1. High Compression ratio $\eta = \dfrac{n}{n_{liquid}} \sim 10^3 - 10^4$

$$n_{liquid} = 4.5 \text{ x } 10^{22} \text{ cm}^{-3}$$

$$(\rho \sim 0.2 \text{ gm/cm}^3)$$

2. Pellet energy gain $G = \dfrac{E_{fusion}}{E_{driver}}$

3. Pre-heat problems

4. Rayleigh-Taylor Instability

5. Uniform Illumination-Complicated Optics

Implosion Laser-Fusion	MICF
Confinement time τ $\tau = \frac{R}{C_s} = \tau_d$ R = Radius of pellet C_s = Sound speed in plasma τ_d = Disassembly time	$\tau = \frac{d}{U_s}$ d = Thickness of metal shell U_s = Sound speed in shell $U_s \sim \sqrt{\frac{T}{\rho}}$ T = Temp in shell much less than that in plasma due to magnetic insulation P = Density of shell much larger than that of plasma due to large atomic mass

$\therefore\ U_s \ll C_s$

$\therefore\ \tau \gg \tau_d$

In fact $\tau_{MICF} = 10^2\ \tau_d \Rightarrow$
I) lower plasma density
II) lower laser energy
III) better coupling to plasma
IV) higher gain

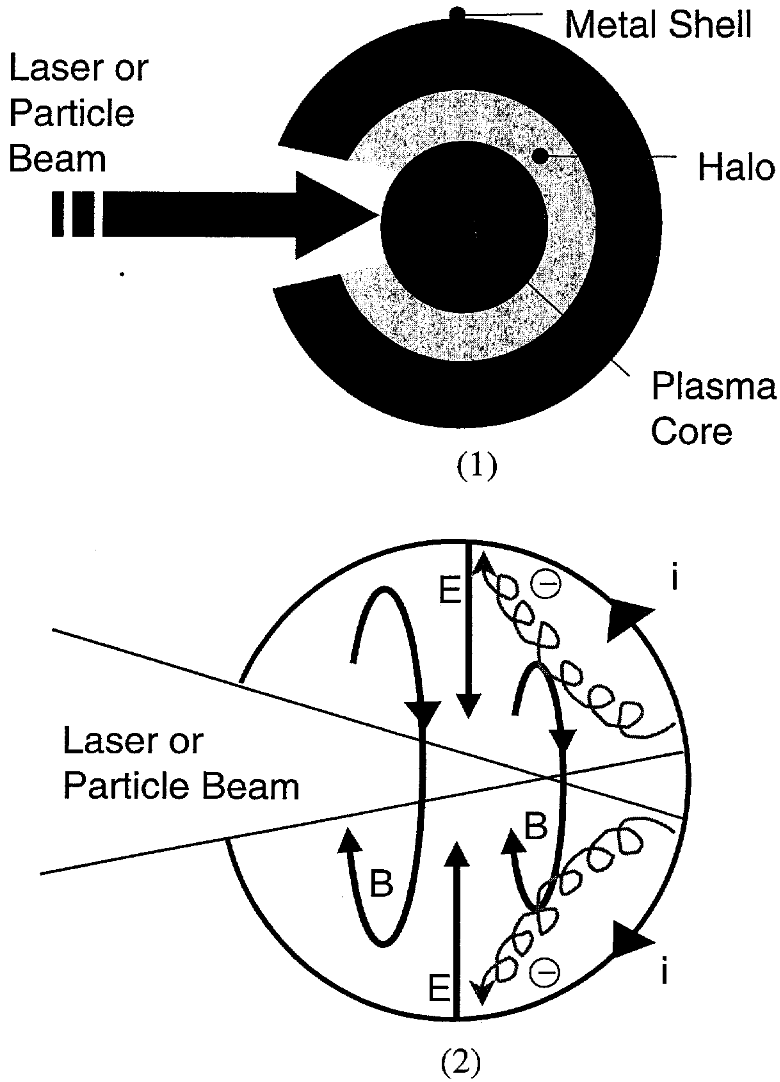

Figure 1: Schematic of (1) Plasma Formation and (2) Magnetic Field Formation in MICF

Main Features of MICF Fusion

1. Combines the favorable aspects of Inertial and Magnetic Fusions into one

2. Physical Containment of plasma is provided by a Metallic shell (e.g. tungsten or gold), and thermal Insulation of plasma energy is provided by a self-generated, strong magnetic field

3. Magnetic Field generation is due to $\nabla n \times \nabla T$ i.e. density and temperature gradients perpendicular to one another.

Generalized Ohm's Law shows that

$\nabla n \times \nabla T \Rightarrow$ Electric field, E $\Rightarrow$ time varying magnetic field, B

4. Decay time of Magnetic Field > plasma confinement time

Plasma Modeling and Basic Equations

1. Examples of particle and energy balance equations for species in MICF; Each species is treated as an Ideal Gas. For DT Fuel Ions in the core

2. Particle Balance Equation

$$\frac{d}{dt}\left\{\frac{4}{3}\pi r^3 n_f\right\} = -\frac{4}{3}\pi r^3\left\{\frac{1}{2}n_f^2 < \sigma v >\right\} + 4\pi r^2\left\{\Gamma_r - \Gamma_f\right\}$$

3. Energy Balance Equation

$$\frac{d}{dt}\left\{\frac{\frac{4}{3}\pi r^3}{\gamma - 1} n_f T_f\right\} + 4\pi r^2 n_f T_f \frac{dr}{dt} = \frac{4}{3}\pi r^3\left\{\frac{3}{2}\frac{n_f n_e}{(n\tau)_{ef}}\left(T_e - T_f\right) + \frac{3}{2}\frac{n_f n_\alpha}{(n\tau)_{\alpha f}}\left(T_\alpha - T_f\right)\right.$$

$$\left. + n_f \sum_{k=1}^{k_{max}} n_k \left(\frac{dE_k}{dt}\right)_f - \frac{3}{4} n_f^2 T_f < \sigma v >_f\right\}$$

$$+ 4\pi r^2\left\{W_r - W_f\right\}$$

4. Γ's and W's are particle and energy fluxes across the magnetic field

5. γ = ratio of specific heats = $5/3$

Electron Balance Equations in the Core

1. Particle Balance

$$n_e = n_f + 2\left(n_\alpha + n_{f\alpha}\right)$$

2. Energy Balance

$$\frac{d}{dt}\left\{\frac{4}{3}\frac{\pi r^3}{(\gamma-1)} n_e T_e\right\} + 4\pi r^2\, n_e T_e \frac{dr}{dt} =$$

$$\frac{4}{3}\pi r^3 \left\{\frac{3}{2}\frac{n_e n_f}{(n\tau)_{ef}}\left(T_f - T_e\right) + \frac{3}{2}\frac{n_e n_\alpha}{(n\tau)_{e\alpha}}\left(T_\alpha - T_e\right)\right.$$

$$\left. + n_e \sum_{k=1}^{k_{\max}} n_k \left(\frac{dE_k}{dt}\right)_e - P_{BC}\right\}$$

$$+ 4\pi r^2 \left\{\Gamma_r E_{re} - \left(\Gamma_f + 2\Gamma_\alpha\right) E_{Le}\right\}$$

where

E_{re} = average energy of an electron diffusing across the magnetic field into the core

E_{Le} = average energy of an electron diffusing out

P_{BC} = Bremsstrahlung Radiation

$$= (3.340x10^{-15}) n_e T_e^{1/2} \left[n_f + 4(n_\alpha + \sum_{k=1}^{k_{max}} n_k) \right] \frac{keV}{cm^3 . sec}$$

Classical and Anomalous Cross Field Transport

1. Particle and Energy Fluxes

i) Particle Flux $\Gamma = -D\frac{\partial n}{\partial r}$

where D = diffusion coefficient

$\frac{\partial n}{\partial r}$ = density gradient

ii) Energy Flux W = $\bar{E}\Gamma$, where $\bar{E}$ = mean particle energy

2. Classical Diffusion

$D = \rho^2 \nu$; ρ = Larmor radius, ν = Collision frequency

3. Anomalous Diffusion

i) Bohm diffusion $D_B = \frac{T}{16eB}$

e = electronic charge
B = Magnetic field strength

ii) Modified Bohm

$$D = \frac{\gamma}{k_\perp^2} = \frac{\gamma}{r^2}; \gamma = \frac{\sqrt{2}}{3} W_D; W_D$$ =drift frequency

Preliminary Results and Fusion Energy Gain

1. For most parameter ranges, the gain "Q" is larger for classical diffusion than for Bohm

2. "Modified Bohm" however appears to yield highest gain; reaching a value of Q = 2623 at an input energy E_{in}=1.15 MJ. This may be attributed to more efficient fueling of the core without degrading its temperature when "mild turbulence" exists in the system

3. The large Q values are reached when the "halo" region is totally depleted. This occurs at about 20 ns into the burn at which time the pressure in the core reaches its maximum

4. The Bremsstrahlung radiation emitted by the core electron plays an important role in ionizing the fuel in the halo region and in the inner regions of the metal shell. This contributes to the pressure build up outside the core which in turn compresses the core increasing its density and fusion energy production.

5. The Gain generally increased as the input energy E_{in} is decreased, although there seems to exist a "cut-off" input energy below which Q becomes very small!

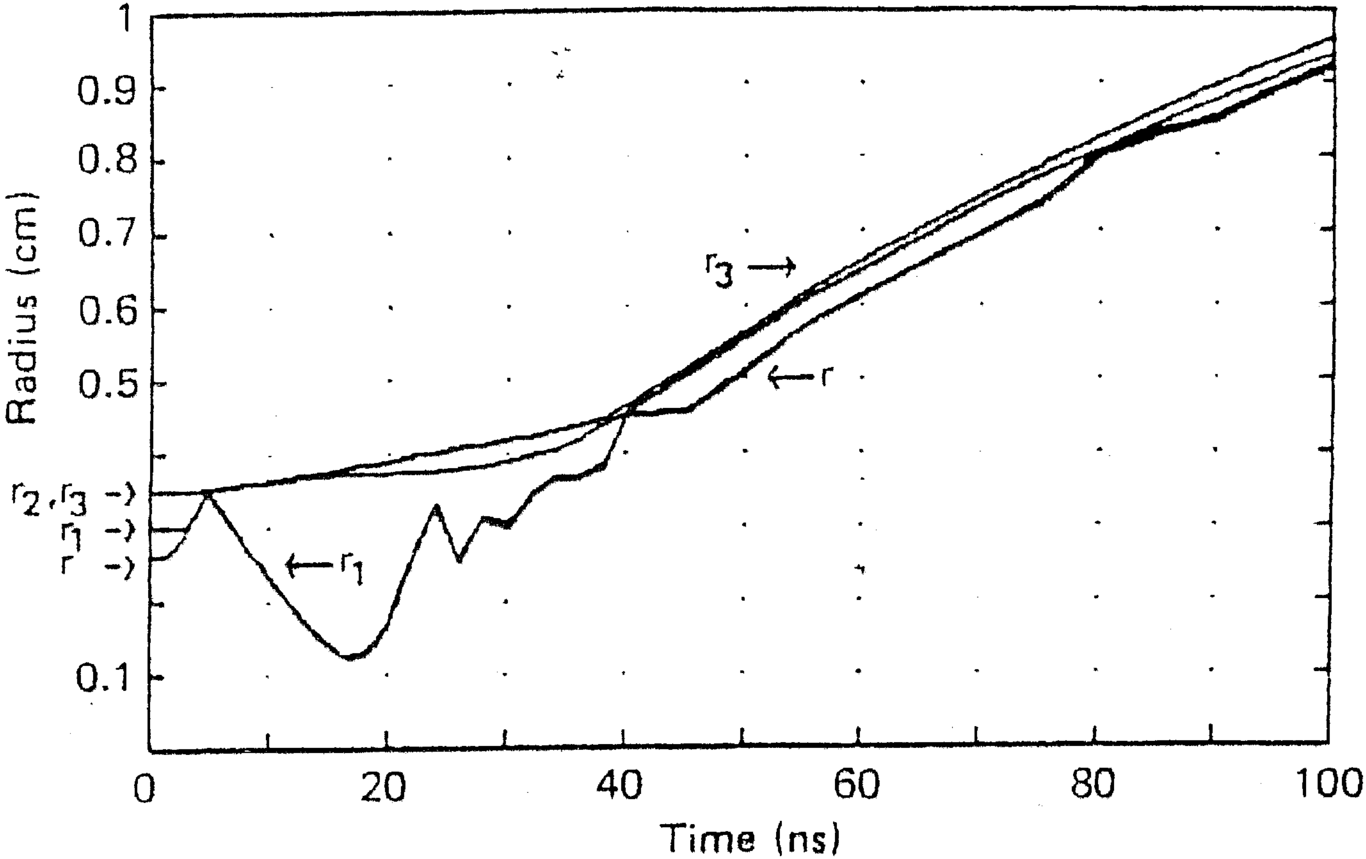

Radii r, r_1, r_2 and r_3 versus time for $E_{in} = 4.033$ MJ.
$B = 100$ T, $N_0 = 5 \times 10^{21}$ cm^{-3}, $T_0 = 20$ keV, classical diffusion.

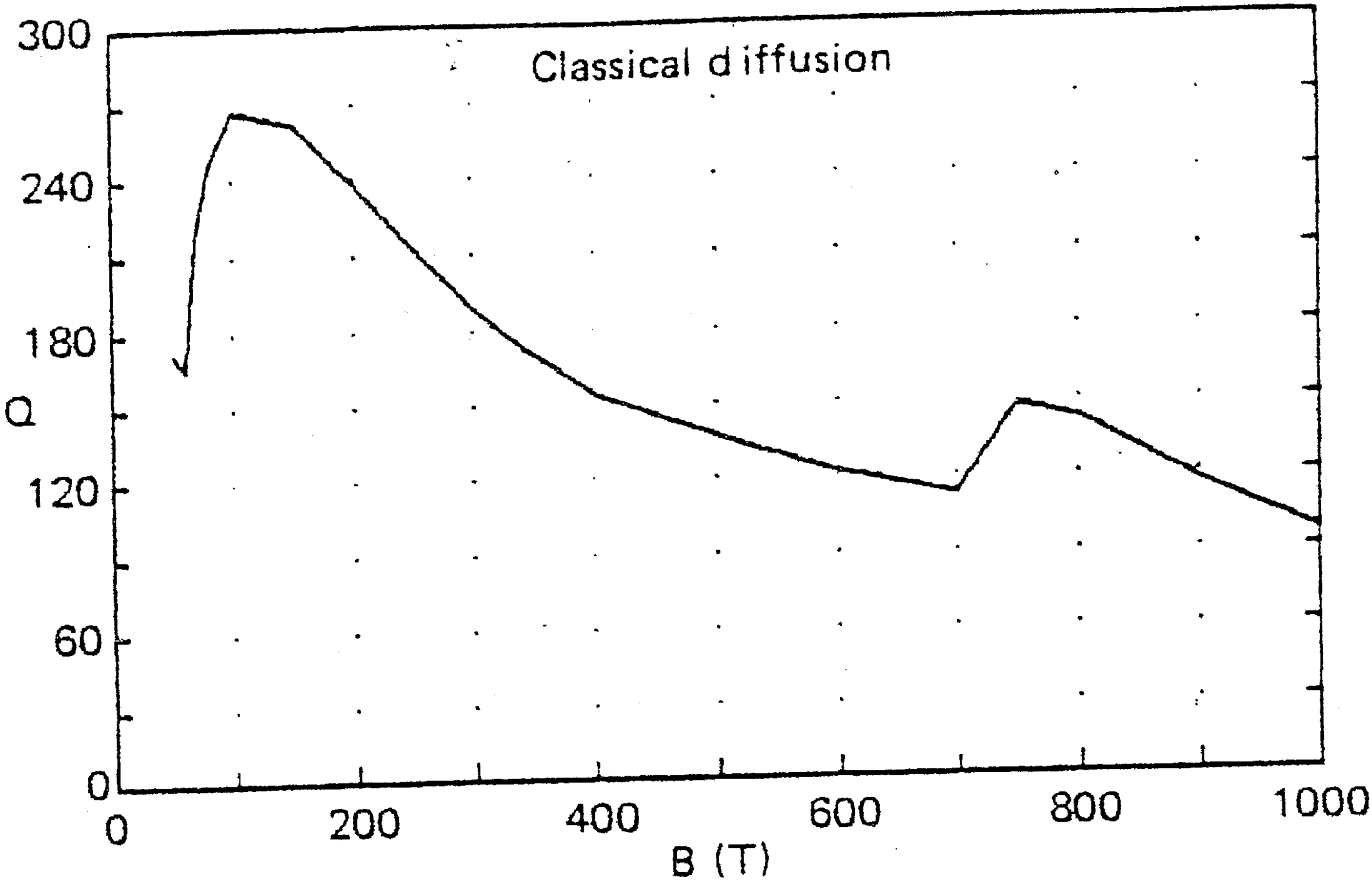

Gain Q versus magnetic field B. $E_{in} = 4.907$ *MJ*, $N = 5 \times 10^{21}$ cm^{-3}, $r_0 = 0.25$, $r_f = 0.3$, $r_{max} = 1$ *cm.*

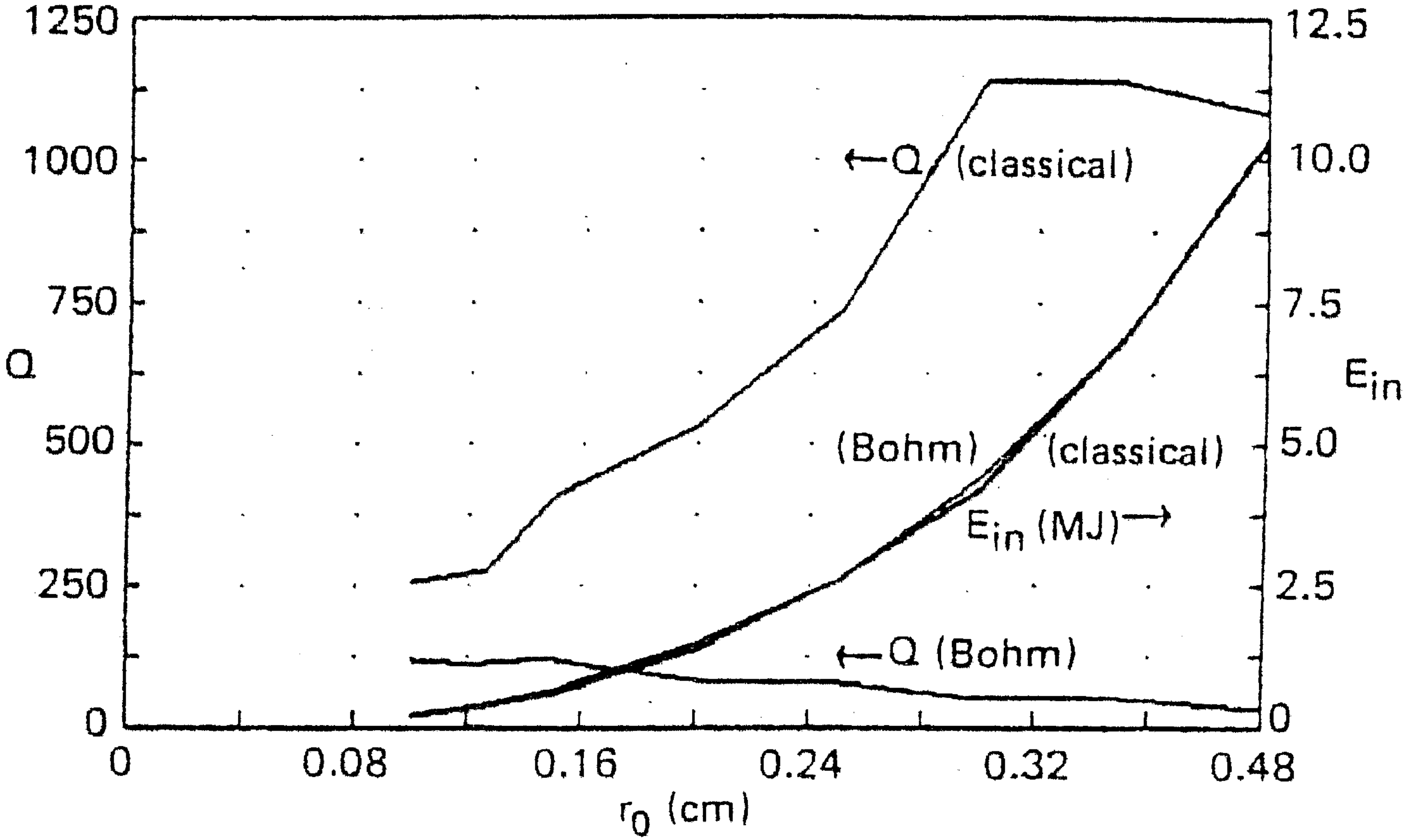

Cut-off input energy E_{in} and gain Q versus initital cavity radius r_0. $B = 100$ T, $N_0 = 5 \times 10^{21}$ cm^{-3}.

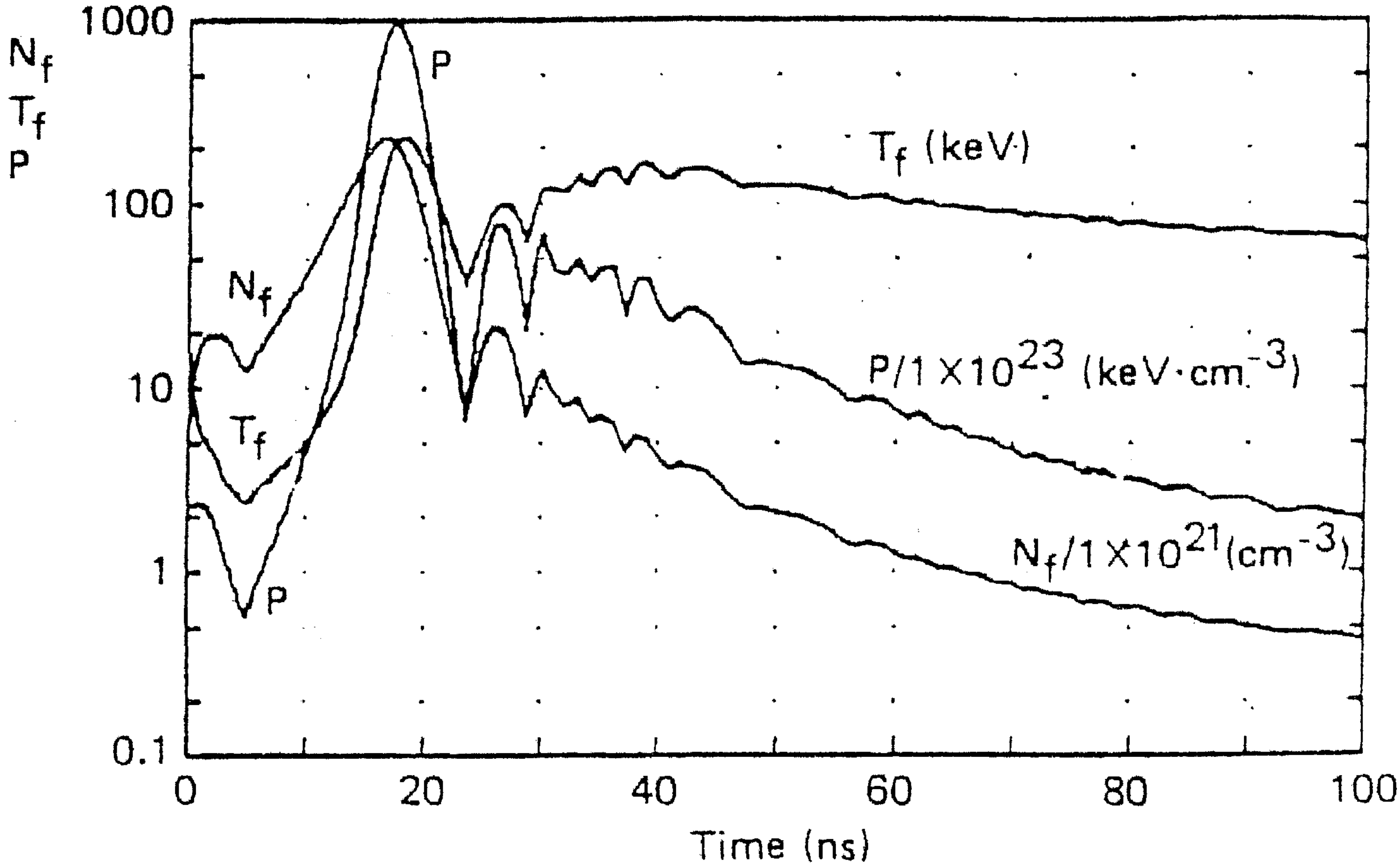

Fuel properties versus time for E_{in} = 4.033 MJ.
B = 100 T, r_0 = 0.25 cm, N = 5 × 10^{21} cm^{-3}, T_0 = 20 keV.

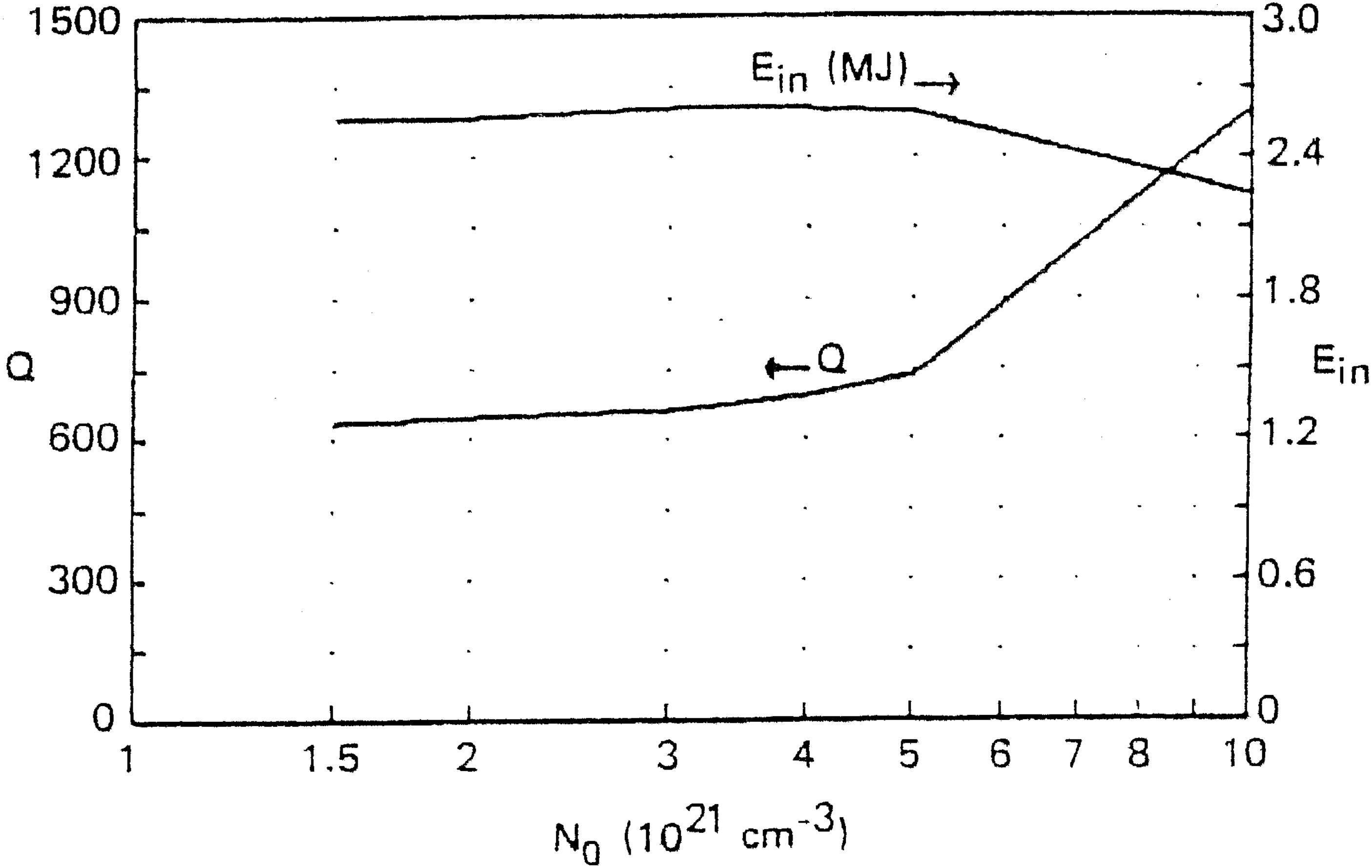

Cut-off input energy E_{in} and gain Q versus initial plasma density N_0. $B = 100$ T, initial cavity radius $r_0 = 0.25$ cm.

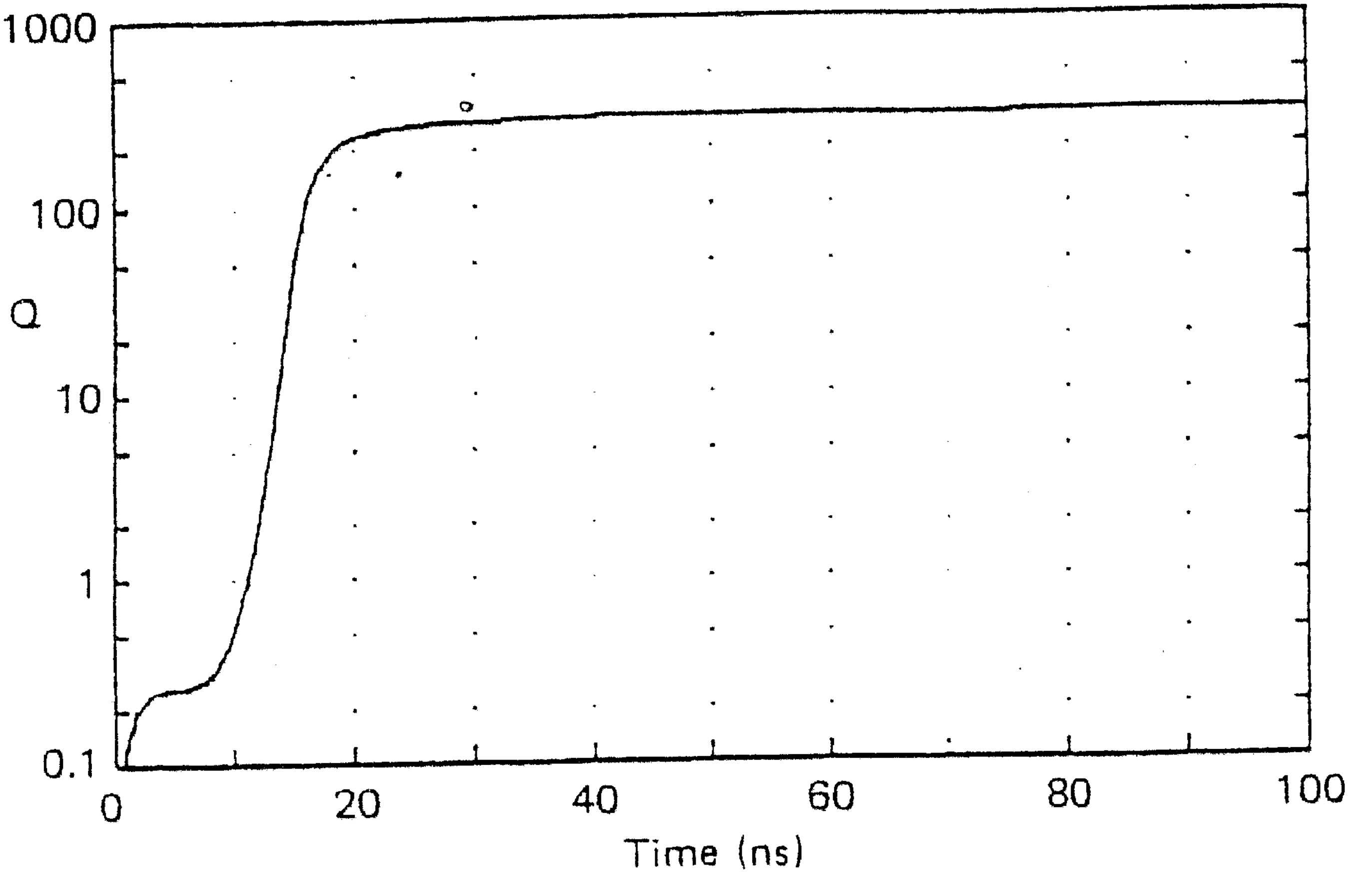

Gain Q versus time for E_{in} = 4.033 MJ. B = 100 T, $N_0 = 5 \times 10^{21}$ cm^{-3}, T_0 = 20 keV, classical diffusion.

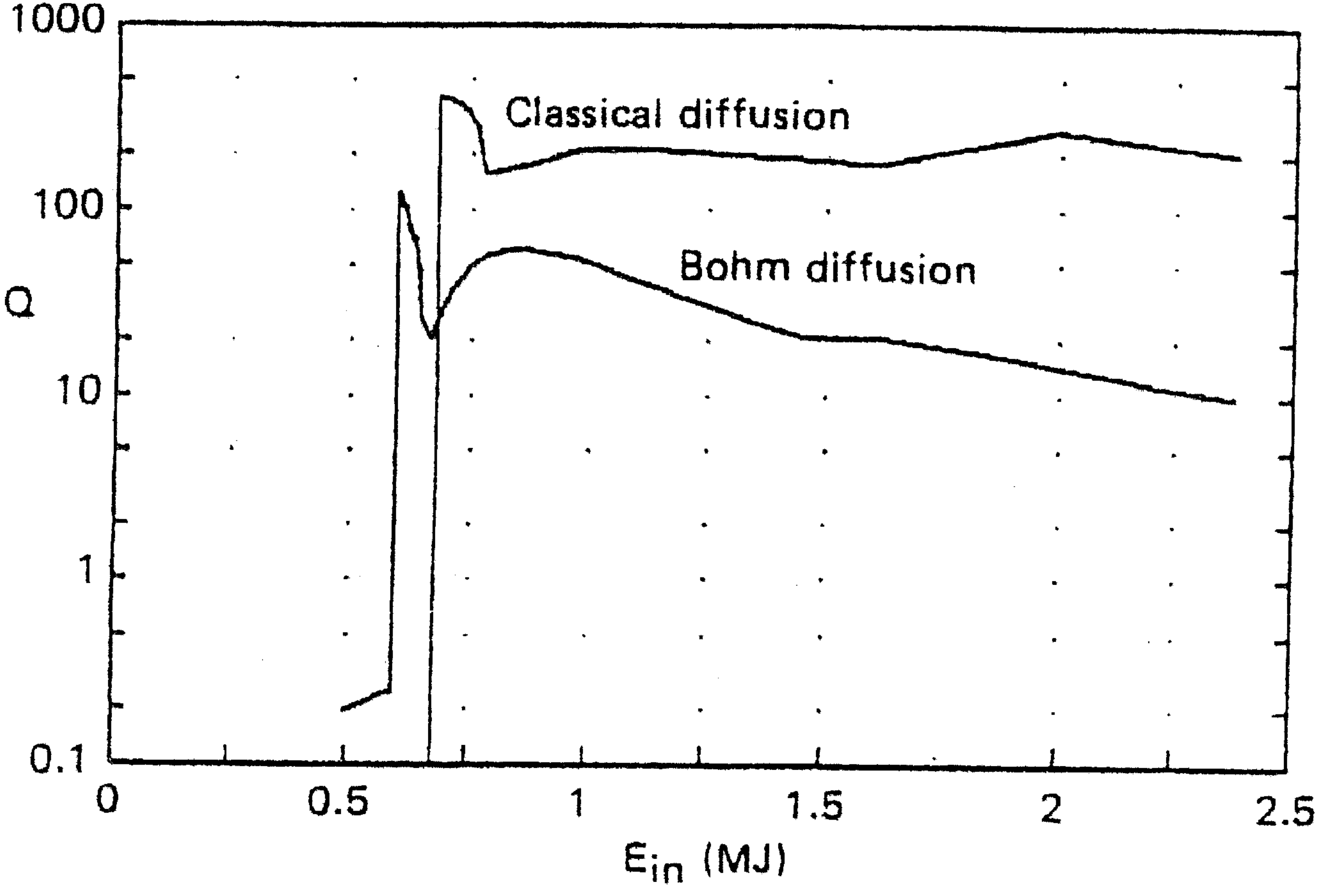

Gain Q versus input energy E_{in}. $B = 100$ T, $N = 5 \times 10^{21}$ cm^{-3}, $r_0 = 0.15$ cm, $r_f = 0.18$ cm, $r_{max} = 0.6$ cm.

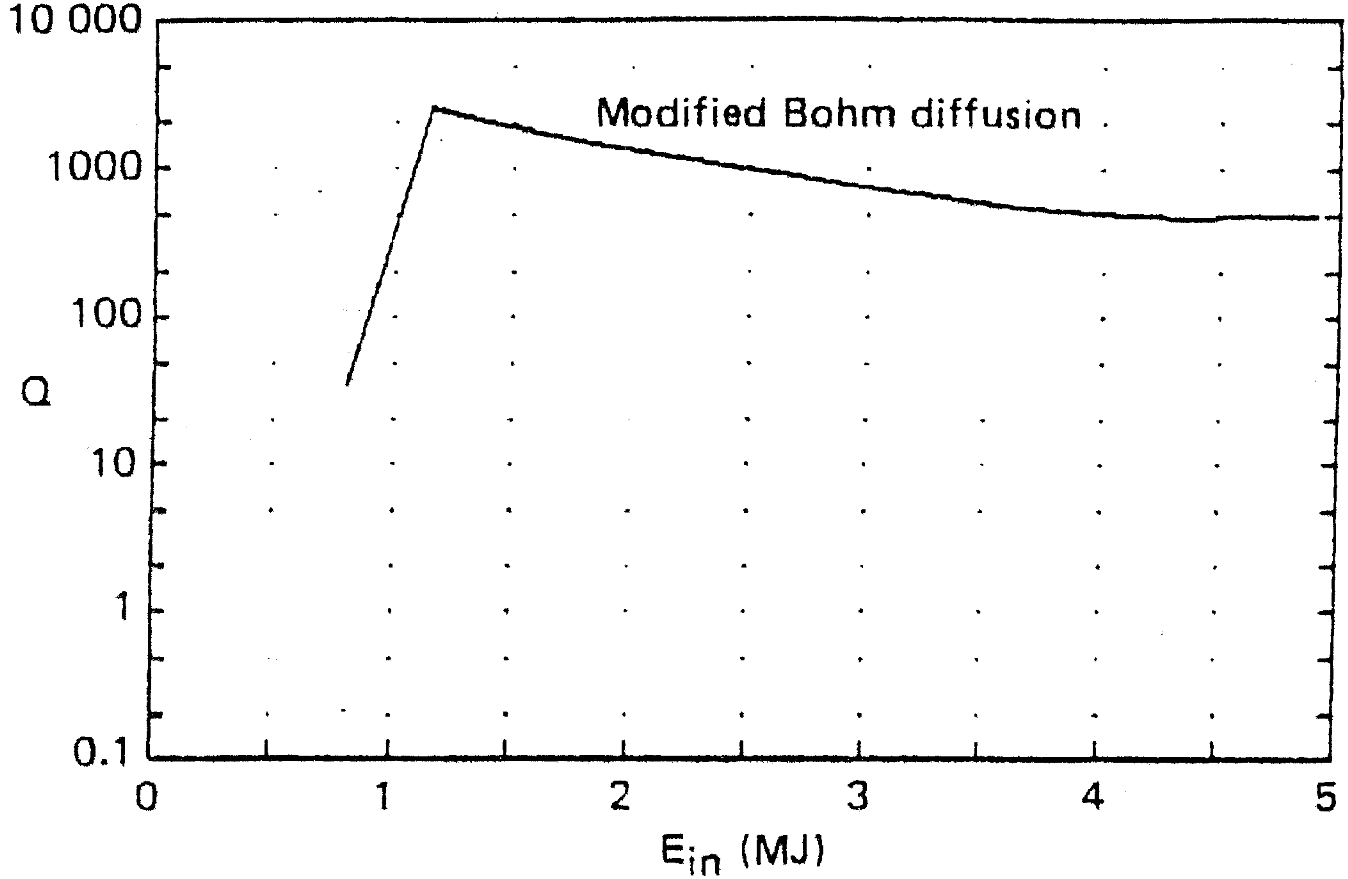

Gain Q versus input energy E_{in} for modified Bohm diffusion. Initial $N = 5 \times 10^{21}\ cm^{-3}$, $r_0 = 0.25$ cm, $r_f = 0.3$ cm, $r_{max} = 1$ cm.

MICF FUSION PROPULSION SYSTEM

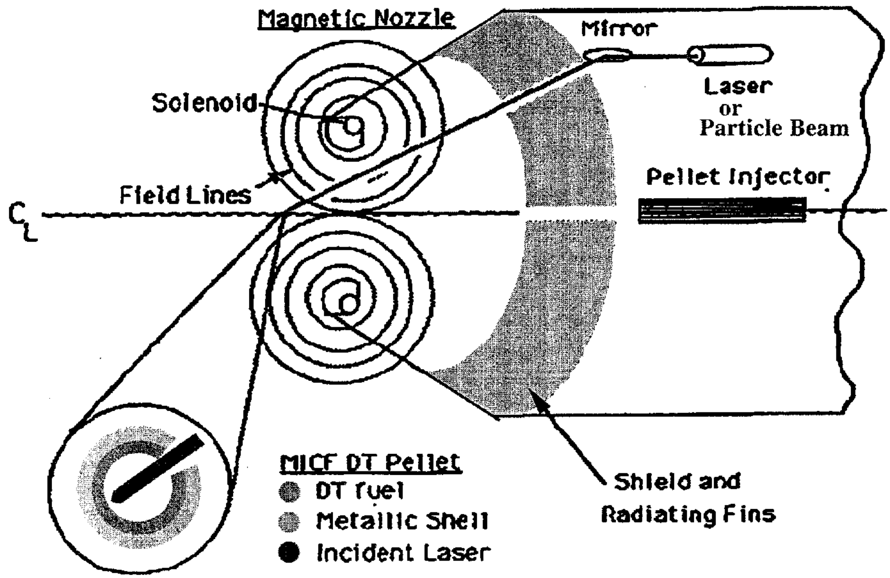

MICF-Driven Rocket

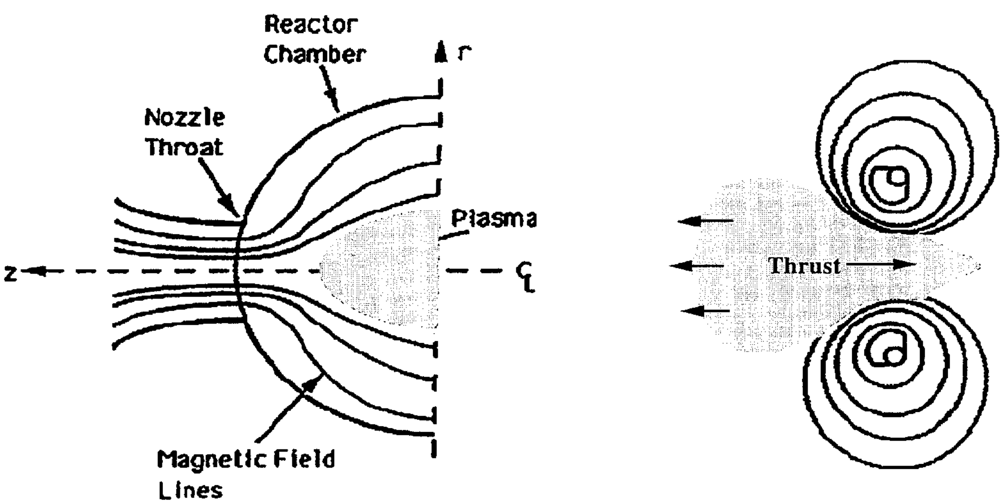

SCALE OF THE HELIOSPHERE AND THE LOCAL INTERSTELLAR MEDIUM

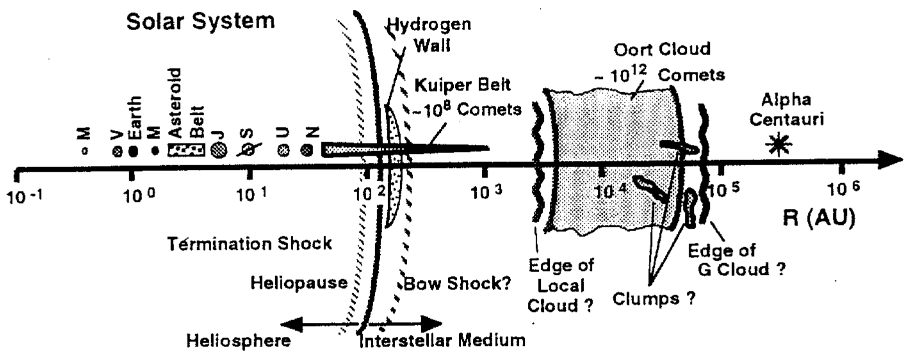

(Mewaldt, 1998)

Application To Propulsion

Table 1
Interstellar Missions with MICF

$I_{sp} = 1.3 \times 10^5$ Sec $\quad F = 4.6 \times 10^4$ N

	conservative	Q = 1911	optimistic	Q = 2623
Mission	trip time	amount of $\bar{p}$' s	trip time	amount of $\bar{p}$' s
Oort FB	37 y	102 gm	8.47 y	23 gm
Oort Rend	41 y	114 gm	10.44 y	29 gm
Oort Rd trip	155 y	427 gm	36.74 y	101 gm
α Centauri FB	968 y	2.67 kg	213 y	587 gm
α Centauri Rend	988 y	2.73 kg	224 y	619 gm
α Centauri Rd trip	3899 y	10.76 kg	872 y	2.41 kg

Table 2
Interplanetary Missions with MICF

Mission	Trip Time	Propellant Mass, m_p	Amount of $\bar{p}$' s
Mars FB	10 d	30 mT	74 mg
Mars Rend	15 d	45 mT	112 mg
Mars Rd trip	31 d	94 mT	234 mg
Jupiter FB	32 d	97 mT	243 mg
Jupiter Rend	46 d	138 mT	345 mg
Jupiter Rd trip	102 d	309 mT	774 mg
Pluto FB	123 d	373 mT	932 mg
Pluto Rend	172 d	520 mT	1.30 gm
Pluto Rd trip	445 d	1345 mT	3.36 gm

Proposed Phase II Investigations

To verify the confinement properties of MICF as formulated in Phase I study:

1 - To experimentally verify the generation of magnetic fields in MICF targets using the facilities of the world class "Ultra Fast" Laboratory at the University of Michigan which can deliver laser beam intensities of > 10^{20} W/cm^2 on target

2 - To measure the magnetic field in a typical target and compare with theoretical predictions

3 - To demonstrate experimentally the confinement dependence on type of metal shell; on thickness of shell and on the strength of the magnetic field

4 - To investigate above phenomena with a particle beam e.g. a proton beam generated by a laser beam impinging on aluminum foil. Experiments at U of M have shown that a laser beam of intensity of 10^{18} W/cm^2 striking a 3μm thick foil gives rise to 10^{10} - 10^{12} protons with average energy of 0.5 MeV

5 – Utilize above information for eventual use of an antiproton beam (10^{12} $\bar{p}'s$ at 20 keV with pulse length of 10's of μs) from trap developed at MS FC to generate fusion-grade plasma in MICF targets

Experimental Magnetic Field Verification

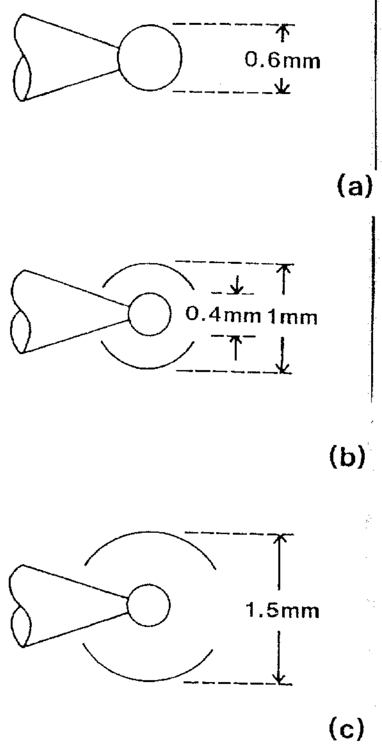

Hole Diameter: 0.6 × Shell Diameter

Larmor Diameter=340μm, if B=100T.

$T_e = 15$ keV

$$\frac{B}{MG} = 3.6\left(\frac{T}{1\,\text{keV}}\right)^{1/2}\left(\frac{10\,\mu m}{d}\right)\left[\frac{A^{1/2}(Z+1)^{-1/2}}{1.1}\right]$$

DT plasma, $A/Z = 2.5$

d = Spot diameter

<u>Note</u> if

$d = 10\,\mu m$

$T = 1$ keV

$B \approx 3.6$ MG

2) $T = 10$ keV

$B \approx 10$ MG

Field Decay time

$$\tau = \frac{\pi \sigma L^2}{c^2}$$

L = Scale Length

σ = Plasma Conductivity

Particle Beam Driven MICF

Incident Laser Beam Intensity ~ 10^18 W/cm^2